ADVANCED MATERIALS
www.advmat.de

Tough and Water-Insensitive Self-Healing Elastomer for Robust Electronic Skin

*Jiheong Kang, Donghee Son, Ging-Ji Nathan Wang, Yuxin Liu, Jeffrey Lopez, Yeongin Kim, Jin Young Oh, Toru Katsumata, Jaewan Mun, Yeongjun Lee, Lihua Jin, Jeffrey B.-H. Tok, and Zhenan Bao**

An electronic (e-) skin is expected to experience significant wear and tear over time. Therefore, self-healing stretchable materials that are simultaneously soft and with high fracture energy, that is high tolerance of damage or small cracks without propagating, are essential requirements for the realization of robust e-skin. However, previously reported elastomers and especially self-healing polymers are mostly viscoelastic and lack high mechanical toughness. Here, a new class of polymeric material crosslinked through rationally designed multistrength hydrogen bonding interactions is reported. The resultant supramolecular network in polymer film realizes exceptional mechanical properties such as notch-insensitive high stretchability (1200%), high toughness of 12 000 J m^{-2}, and autonomous self-healing even in artificial sweat. The tough self-healing materials enable the wafer-scale fabrication of robust and stretchable self-healing e-skin devices, which will provide new directions for future soft robotics and skin prosthetics.

Electronic (e-) skin is a form of wearable electronics with skin-mimetic mechanical and sensing properties.[1–3] Efforts to render e-skin devices robust and durable to withstand mechanical damage have led to reports of self-healing electronic polymers.[4–10] Unfortunately, since most self-healing polymers are based on weak dynamic bonds, they easily break along locations where damage is incurred due to their low fracture energies typically at ≈100 J m^{-2} or less. Furthermore, most self-healing polymers are highly viscoelastic with weak mechanical toughness and are susceptible to fatigue under large deformation. Tough, self-healable, and stretchable materials are needed for practical e-skin devices. We report herein a new class of silicone polymer material crosslinked through controlled multistrength hydrogen bonding interactions. The self-healable elastic polymer network exhibits an extremely high fracture energy (≈12 000 J m^{-2}) and notch-insensitive stretching up to 1200%. It is readily moldable and stackable into any stretchable 3D object shapes. We further illustrate its application through the fabrication of highly stretchable and tough self-healing e-skin devices. Our simple polymer design concept allows a broad range of mechanical property tuning to be desirable for targeted applications.

Briefly, the underlying principle for our tough and self-healable film is achieved through the spontaneous formation of a mixture of both strong and weak crosslinking hydrogen bonds. The strong crosslinking bonds confer robustness and elasticity, while the weak bonds are able to dissipate strain energy through efficient reversible bond breakage and reformation. Our film is easily integrated with EGaIn (liquid metal) alloy, in which we proceed to fabricate a new generation of e-skin: highly tough and stretchable self-healing strain sensor that is able to sense a wide range of human motions and withstand constant mechanical damage. The described approach is also easily scalable, in which we demonstrated a wafer-scale 7 × 7 strain sensor array that is able to sense strain deformations induced by external stimuli. Our fabricated robust and stretchable self-healing e-skin will provide new capabilities and facile fabrication methods for future soft robotics and skin prosthetics.[1]

Recently, significantly toughened elastomers with improved stretchability have been realized by incorporating sacrificial bonds through sequential polymerizations within a triple molecular network.[11] However, rupturing of the sacrificial molecular network results in "irreversible" damage to the elastomer after the initial stretch. To enable recoverable mechanical properties, reversible energy dissipation mechanism is needed. Indeed, such systems have been used for tough hydrogel designs.[12,13] Such a concept is only recently applied to other elastomers.[14–18] For example, Guan et al. introduced noncovalent sacrificial bonds into a covalent polymer network and observed significantly enhanced ductility and toughness. Furthermore, our group reported a supramolecular elastomer crosslinked by three kinds of dynamic metal–ligand interactions

Dr. J. Kang, Dr. D. Son, G.-J. N. Wang, Y. Liu, Dr. J. Lopez, Y. Kim, Dr. J. Y. Oh, Dr. T. Katsumata, J. Mun, Dr. Y. Lee, Prof. L. Jin, Dr. J. B.-H. Tok, Prof. Z. Bao
Department of Chemical Engineering
Stanford University
443 Via Ortega, Stanford, CA 94305, USA
E-mail: zbao@stanford.edu
Dr. D. Son
Biomedical Research Institute
Korea Institute of Science and Technology
5 Hwarang-ro 14-gil, Seongbuk-gu, Seoul 02791, South Korea
Prof. L. Jin
Department of Mechanical and Aerospace Engineering
University of California
Los Angeles, CA 90095-1597, USA
The ORCID identification number(s) for the author(s) of this article can be found under https://doi.org/10.1002/adma.201706846.

DOI: 10.1002/adma.201706846

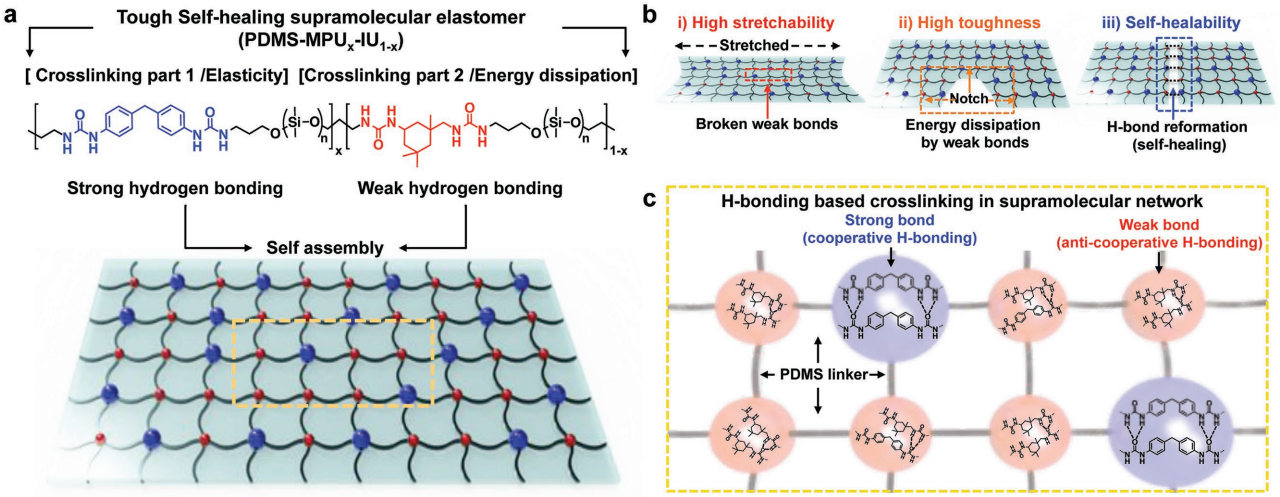

Figure 1. Molecular design of the supramolecular elastomer with high toughness, stretchability, and self-healing property. a) Chemical structure of PDMS–MPU$_x$–IU$_{1-x}$ and the proposed ideal supramolecular structure. b) Schematics of a stretched polymer film (left), notched film (middle), and healed film (right). c) Possible hydrogen bonding combinations for strong bond and weak bond, respectively.

in a crosslinking bond and realized self-recoverable energy dissipation. Such a reversible energy dissipation system is also needed for autonomous self-healing. However, the applications of self-healing materials in electronics have so far been limited to simple demonstrations of conductors and wires largely due to their significant viscoelasticity, moisture, and water sensitivity for H-bonding-based materials or issues with mobile ions for metal–ligand-based materials. To address the above-mentioned shortcomings, we describe here a new polymer design strategy, based on self-sorting chemistry, to achieve unprecedented supramolecular network composed of a varying composition of well-defined strong and weak hydrogen bonds. Our synthesized supramolecular structure is observed to realize all the desired attributes, namely, high stretchability, exceptional toughness, and underwater self-healablility (**Figure 1**).

Specifically, we synthesized a series of polymers through a one-pot polycondensation reaction between bis(3-aminopropyl)-terminated poly(dimethylsiloxane) (H_2N–PDMS–NH_2, M_n = 5000) and a mixture of 4,4′-methylenebis(phenyl isocyanate) and isophorone diisocyanate. As a result, the PDMS oligomers (PDMS–MPU$_x$–IU$_{1-x}$) were linked by 4,4′-methylenebis(phenyl urea) (MPU unit) and isophorone bisurea units (IU unit) with varied ratios of MPU and IU units (structures shown in Figure 1 and Figure S1 in the Supporting Information). PDMS and hydrogen bonding are chosen for the modifications because they are known to be biocompatible and contain no toxic elements, therefore, making this an ideal carrier material for e-skin devices and components.

All the PDMS–MPU$_x$–IU$_{1-x}$ polymers were able to form colorless and transparent film on octadecyltrimethoxysilane (OTMS)-treated substrates to allow easy release into free-standing films (see Supporting Information and Figure S2 therein). The PDMS–MPU$_{0.4}$–IU$_{0.6}$ film could be stretched to 16 times its original length at a loading rate of 2 min^{-1} without rupturing (**Figure 2**a,b). When the film was stretched slower, it exhibited higher stretchability (Figure S4, Supporting Information). Our polymer film showed the good stability under ambient conditions (Figure S4, Supporting Information). Most remarkably, our polymer film was able to achieve notch-insensitive stretching up to 1200% strain, that is, when a big notch of ≈2–3 mm was introduced in the 5 mm width film and pulled to 1200% strain, the notch was blunted and did not tear further, demonstrating its exceptional toughness (Figure 2d; Figure S3, Supporting Information). In comparison, typical PDMS (sylgard 184) substrates rupture at less than 200% strain. Other commonly used e-skin substrates, such as polyurethane, and SEBS rupture at 700% and 280% strain, respectively. Moreover, none of them can achieve notch-insensitive stretching more than 150% strain, indicating much lower toughness and fracture tolerance (Table S1, Supporting Information).

To investigate the origin of the remarkable mechanical properties of the PDMS–MPU$_x$–IU$_{1-x}$, we proceed to synthesize their "parent" polymers (PDMS–MPU and PDMS–IU), which consist of only one single type of crosslinking hydrogen bond. The Young's modulus of the PDMS–MPU film was calculated to be 0.98 MPa from its low-strain region and its strain at break was 750% (Figure 2b; Table S1, Supporting Information). In contrast, PDMS–IU film was not elastic and underwent continuous plastic deformation upon applied strain (Figure 2b; Figure S4 and Table S1, Supporting Information). This reveals that the crosslink strength of MPU–MPU and IU–IU are significantly different. In specific, MPU units are able to form strong bonds to impart elasticity, while the IU units are able to form weak bonds for energy dissipation. The difference in crosslink strength may be attributed to the manner that these noncovalent interaction form. The MPU units can form quadruple hydrogen bonding in a cooperative manner with counter MPU units[19] whereas the IU units can only form maximum dual hydrogen bonding with another IU unit due to the steric hindrance from the isophorone moieties (Figure 1; Figure S1, Supporting Information). Multivalent effect hence results in MPU–MPU interaction being much stronger than IU–IU interaction[19,20] such that the MPU–MPU crosslinking can better hold the elastomer together to impart elasticity.

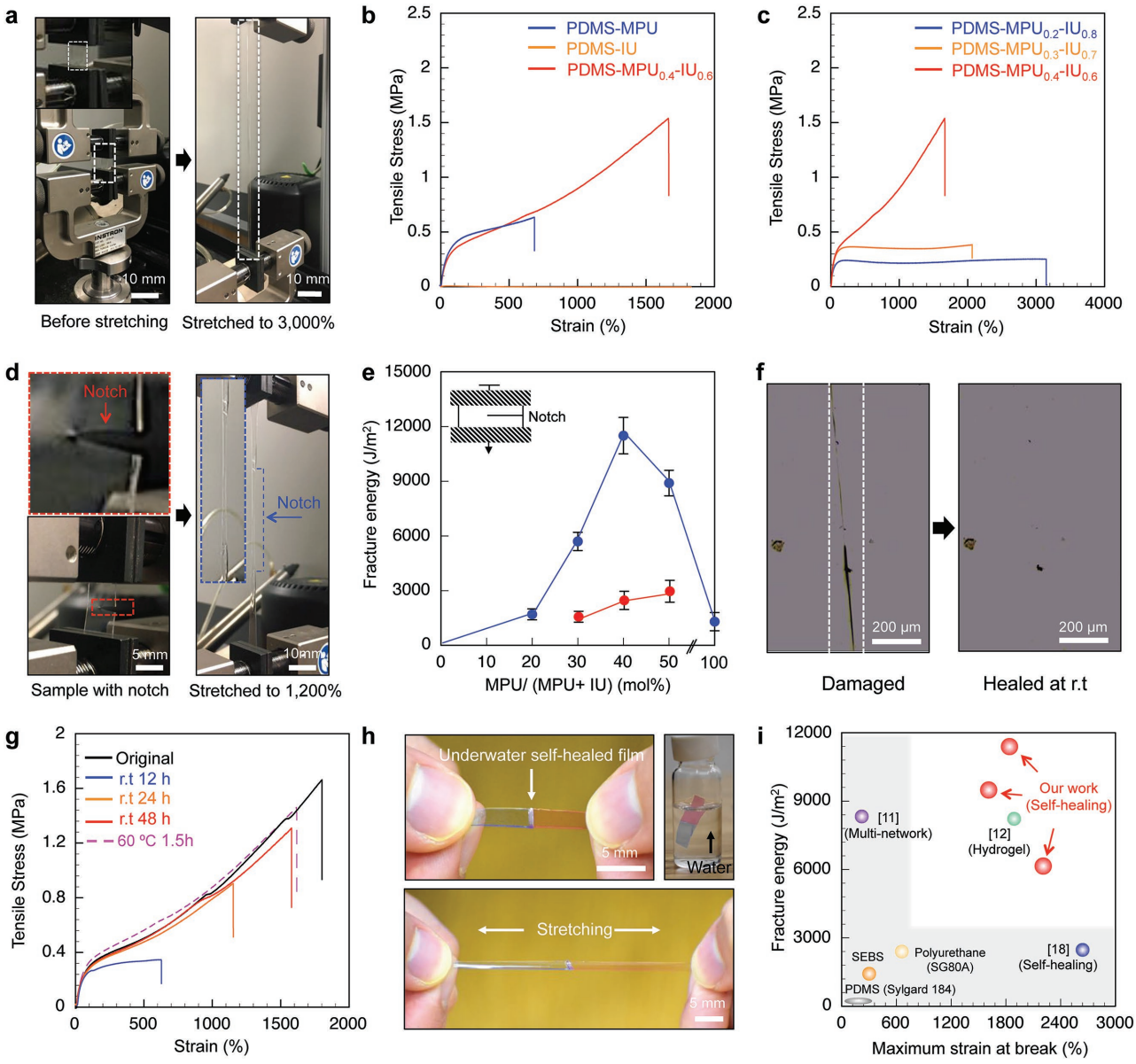

Figure 2. Mechanical and self-healing properties of the PDMS–MPU_x–IU_{1-x} polymer film. a) A PDMS–$MPU_{0.2}$–$IU_{0.8}$ polymer film before stretching (left) and showing high stretchability at 3000% stretching (right) in a Instron machine. b) Stress–strain curves of the films prepared with PDMS–MPU (blue), PDMS–IU (orange), and PDMS–$MPU_{0.4}$–$IU_{0.6}$ (red) with a sample width of 5 mm, a thickness of 0.4–0.5 mm, and a length of 10 mm at a loading rate of 20 mm min^{-1}. c) Stress–strain curves of the films prepared with PDMS–$MPU_{0.2}$–$IU_{0.8}$ (blue), PDMS–$MPU_{0.3}$–$IU_{0.7}$ (orange), and PDMS–$MPU_{0.4}$–$IU_{0.6}$ (red) with a sample width of 5 mm, a thickness of 0.4–0.5 mm, a length of 10 mm, and a loading rate of 20 mm min^{-1}. d) A notched- PDMS–$MPU_{0.4}$–$IU_{0.6}$ polymer film before stretching (left) and after 1200% stretching (right) in an Instron machine showing that the film is notch insensitive. e) Fracture energy as a function of molar ratio of MPU and IU units in polymer (PDMS–MPU_x–IU_{1-x}, blue) and blended film (PDMS–MPU and PDMS–IU, red). f) Optical microscope images of the damaged and healed PDMS–$MPU_{0.4}$–$IU_{0.6}$ film showing disappearance of the scar after healing at 20 °C for 3 d. g) Stress–strain curves of a film healed at room temperature for different lengths of time showing an increase of the stretching ability when the film is allowed to heal for longer. When the film was healed at 60 °C, we observed improved healing process. h) Self-healing of the PDMS–$MPU_{0.4}$–$IU_{0.6}$ film can even take place under water. The PDMS–$MPU_{0.4}$–$IU_{0.6}$ film was bisected to two pieces, where they were stained by pink and blue ink from color pen, respectively, and put together under water for self-healing (top). After 24 h, the film was successfully stretched (bottom). i) A comparison of this work to recent work in synthetic stretchable and tough material. The work of Li et al.[18] and our work exhibit autonomous self-healing property. Sun et al.[12] reported highly stretchable and tough hydrogel.

Particularly, the PDMS–$MPU_{0.4}$–$IU_{0.6}$ film could dissipate strain energy efficiently, as shown by the observed pronounced hysteresis (Figure S5, Supporting Information). The area between the loading and unloading curves represents the energy dissipated per unit volume from mostly the weak hydrogen bond breakage. If the same polymer film was stretched to 1000% strain and released successively, the tensional stresses of the second stretch would be significantly

lower than that of the previous cycle. The same polymer film was then allowed to rest for 30 min and stretched again. The polymer showed complete recovery even after multiple cycles of stretching, as the obtained stress–strain curve was almost identical to that of the first stretching cycle (Figures S5 and S6, Supporting Information). When the polymer films were stretched and kept under that strain for 30 min, they needed a longer time to recover and did not fully return to original dimension (residual strain) (Figure S6, Supporting Information). However, the deformation recovery of the PDMS–$MPU_{0.4}$–$IU_{0.6}$ film after being stretched at low strain region (<40%) is fast and elastic with small hysteresis, which is a desirable property for skin-inspired wearable electronics (Figure S5, Supporting Information). The PDMS–$MPU_{0.4}$–$IU_{0.6}$ film exhibits notch-insensitive stretching and a record-high fracture energy (≈12 000 J m^{-2}) among reported intrinsically tough materials as well as among self-healing polymers (Figure 2d,e,i; Figure S7, Supporting Information).

The mechanical properties of PDMS–MPU–IU depend on the ratio of MPU and IU units. When the ratio of MPU units in the polymer was decreased, the fracture strain of the polymer film was increased but the Young's modulus and fracture energy were decreased (Figure 2b,c,e; Table S1, Supporting Information). For high mechanical strength, a higher MPU–MPU crosslinking density is needed. We believe that the formation of the supramolecular structure in the polymer film is driven by the combination of stronger MPU–MPU bonds and the weaker MPU–IU or IU–IU bonds (Figure 1). In $CHCl_3$ solution, the MPU units were observed to interact primarily with MPU unit rather than IU, which was confirmed by both concentration-dependent viscosity measurements and NMR measurements (Figures S8 and S9, Supporting Information). Such a pre-crosslinked polymer network by MPU–MPU interactions in $CHCl_3$ solution gives rise to a supramolecular structure in the polymer film with both strong bonds and weak bonds upon removal of the solvent. Our resulting supramolecular structure enabled high stretchability and high fracture energy (Figure 1). When a notched sample is stretched, the strong bonds are probably sufficient to block the induced crack propagation while the weak bonds simultaneously break and dissipate strain energy. We hypothesized that the breakage of the weak bonds was able to reduce the stress concentration on the strong bonds in the notch (Figure 1). Moreover, since the MPU and IU units are covalently linked by flexible PDMS, the above process could synergistically take place (Figure 2e, red).

Over the last decade, remarkable progress in self-healing materials has been made through encapsulating healing agents or incorporating dynamic bonds.[21–29] However, most of these studies rely on the input of energy, e.g., heat or light, or additives to induce healing. A few examples of room temperature, i.e., autonomous, self-healing rubbers, were reported.[22,24] However, most of these materials tear easily due to the use of weak dynamic bonds. First, we observed that the scar on the cut polymer film (PDMS–$MPU_{0.4}$–$IU_{0.6}$) almost disappeared after healing at room temperature (r.t.) for 3 d (Figure 2f). The healed polymer film is again able to be stretched to 1500% after 48 h with high self-healing efficiency (78%) (Figure 2g; Table S1, Supporting Information). The healing process can be improved by heating (Figure 2g). Polymers with lower MPU ratios, such as PDMS–$MPU_{0.2}$–$IU_{0.8}$ and PDMS–$MPU_{0.3}$–$IU_{0.7}$ showed faster healing and higher self-healing efficiencies given the same healing time (Table S1, Supporting Information). This observed ambient self-healing property was attributed to the abundant dynamic hydrogen bonds within the elastomer and the low T_g (<0 °C) of PDMS backbone (Figure S10, Supporting Information).[18] The MPU unit was reported previously to have the tendency to aggregate into large domains due to its rigid molecular structure and cooperative H-bonding manner.[21] However, in our system, the incorporation of IU units reduced the probability for MPU units to form large aggregation domains. This is crucial for keeping T_g of the polymer lower than room temperature. Therefore, the IU units are essential not only for energy dissipation during stretching, but also for lower T_g by preventing large aggregations of MPU units.

Second, unlike other self-healing materials based on hydrogen bonding,[22,24] we observed that the self-healing of the PDMS–$MPU_{0.4}$–$IU_{0.6}$ is water insensitive and even heals under artificial sweat. This property is highly relevant to wearable electronics and is previously not possible for self-healing materials. When the severed polymer films were healed in water for 24 h, the resulting film can still be stretched up to 1100% strain (Figure 2h; Figure S11, Supporting Information). To the best of our knowledge, this is the first report of hydrogen-bonding-based elastomer capable of self-healing in water or sweat. We hypothesize that the hydrophobicity of our polymer backbone (PDMS) may increase the enthalpy gain for hydrogen bonding formation, which is responsible for self-healing. The resulting enthalpy gain might exceed entropy gain by hydration of hydrogen bonding units (which will lead to self-healing failure). Importantly, we observed that there is no significant water uptake into the polymer film (Figure S11, Supporting Information). Moreover, we could not see any changes in mechanical properties even after soaking into water or artificial sweat for 24 h (Figure S11, Supporting Information). This suggests a new design strategy for water-insensitive self-healing polymers based on broadly used hydrogen bonding systems. The detailed mechanism for self-healing in water of our elastomer is currently under investigation.

The exceptional mechanical and self-healing properties of PDMS–$MPU_{0.4}$–$IU_{0.6}$ elastomers allow them to be processed in various ways: solution processing or molding and bonding at elevated temperatures and even room temperature (Figure S12, Supporting Information). For example, two sheets of PDMS–$MPU_{0.4}$–$IU_{0.6}$ films can be bonded together giving mechanical properties similar as the bulk film (Figure S13, Supporting Information). Further, PDMS–$MPU_{0.4}$–$IU_{0.6}$ blocks can be readily attached to the PDMS–$MPU_{0.4}$–$IU_{0.6}$ substrate with robust interface even under large applied biaxial strain (Figure S14, Supporting Information). Further, we are able to fabricate 3D self-healable objects, such as self-healing flower (Figure S14, Supporting Information). Moreover, our tough self-healing film can easily be sutured on soft animal skin surfaces without rupturing due to exceptional toughness (Figure S14, Supporting Information). Particularly, most of soft materials utilized for biomedical applications as a substrate cannot be sutured on soft surfaces due to their low fracture toughness (Figure S14, Supporting Information). Combining with its self-healing property in water, this material is especially useful as a substrate for

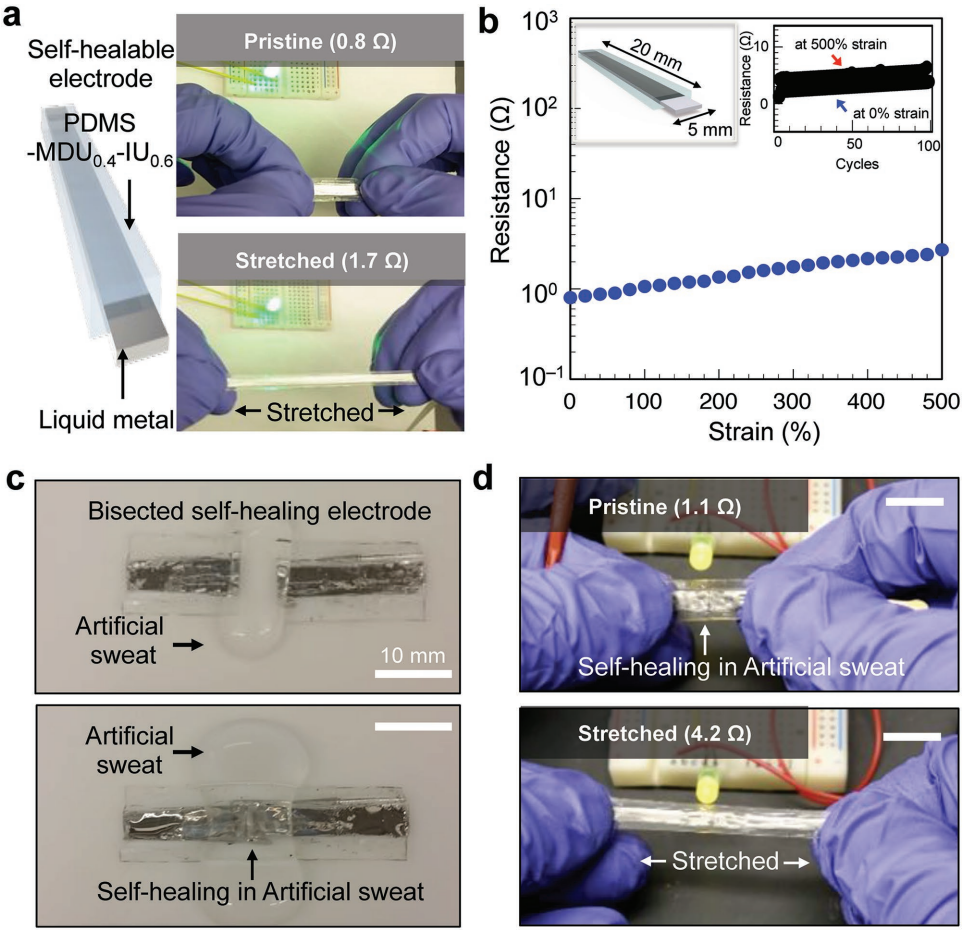

Figure 3. Highly stretchable and self-healable electrode. a) Schematic illustration of self-healing electrode (left). Optical images of self-healing electrode equipped with the light-emitting diode (LED) lamp before stretching (middle) and after stretching (right). b) Electrical resistance as a function of strain with self-healing electrode and electrical resistance under cyclic stretching (inset). c) Self-healing electrode with conductive lines was cut into two pieces (top). They were put together in artificial sweat (bottom). Artificial sweat solution is a potassium phosphate dibasic solution (1.0 M) purchased from Sigma-Aldrich (P8584). d) After 9 h self-healing process in artificial sweat, the electrode was stretched with the LED lamp.

attaching electronics onto soft surfaces (Figure S14, Supporting Information).

Taking advantage of these features, we fabricated stretchable and autonomous self-healing electrodes composed of liquid metal EGaIn[30–32] as a conductive layer and PDMS–$MPU_{0.4}$–$IU_{0.6}$ as the encapsulation and supporting layer (**Figure 3**a). EGaIn has been previously shown as a promising material for fabricating stretchable and self-healing electrodes based on microfluidic device structure.[33,34] Dickey and co-workers demonstrated reconfigurable conductive wires.[4] First, we prepared the polymer film with periodic polymer walls by pressing the film with a Teflon mold at 80 °C (Figure 3a; Figure S15, Supporting Information). EGaIn was then bladed using a small piece of polymer film as a brush on the pattern and encapsulated with the same polymer film through heating for rapid bonding, so that the liquid metal is completely encapsulated. The electrode encapsulated inside two sheets of PDMS–$MPU_{0.4}$–$IU_{0.6}$ exhibits similar mechanical properties as the polymer film stack (Figure S16, Supporting Information).

This electrode exhibited high stretchability (500%) with stable (100 cycles) and reversible low resistance (Figure 3a,b). Importantly, this electrode is self-healable at room temperature even under water. To demonstrate its self-healing in artificial sweat, the electrode was cut into two pieces and put together for self-healing under water condition (Figure 3c). The electrical conductivity was recovered instantaneously when two broken pieces were put in contact. After 12 h of healing under artificial sweat, the electrode is observed to restore its original electrical properties and mechanical properties (Figure 3d; Figure S17, Supporting Information). To the best of our knowledge, this is the first example of a water-insensitive self-healing electrode with a high stretchability of 500% and high conductivity (Figure 3; Figure S17, Supporting Information).

Using our prepared self-healing electrodes, we proceed to fabricate a capacitive strain-sensing e-skin by sandwiching the two electrodes, with tough self-healing polymer film acting as a dielectric layer (**Figure 4**a). Again, the two EGaIn electrodes were sandwiched with the elastomer to enable one overall robust strain sensor with a highly stable interface (Figure S18, Supporting Information). The e-skin could be stretched to five times its original length without losing good contact between layers and its sensing capabilities. The stretchability of our

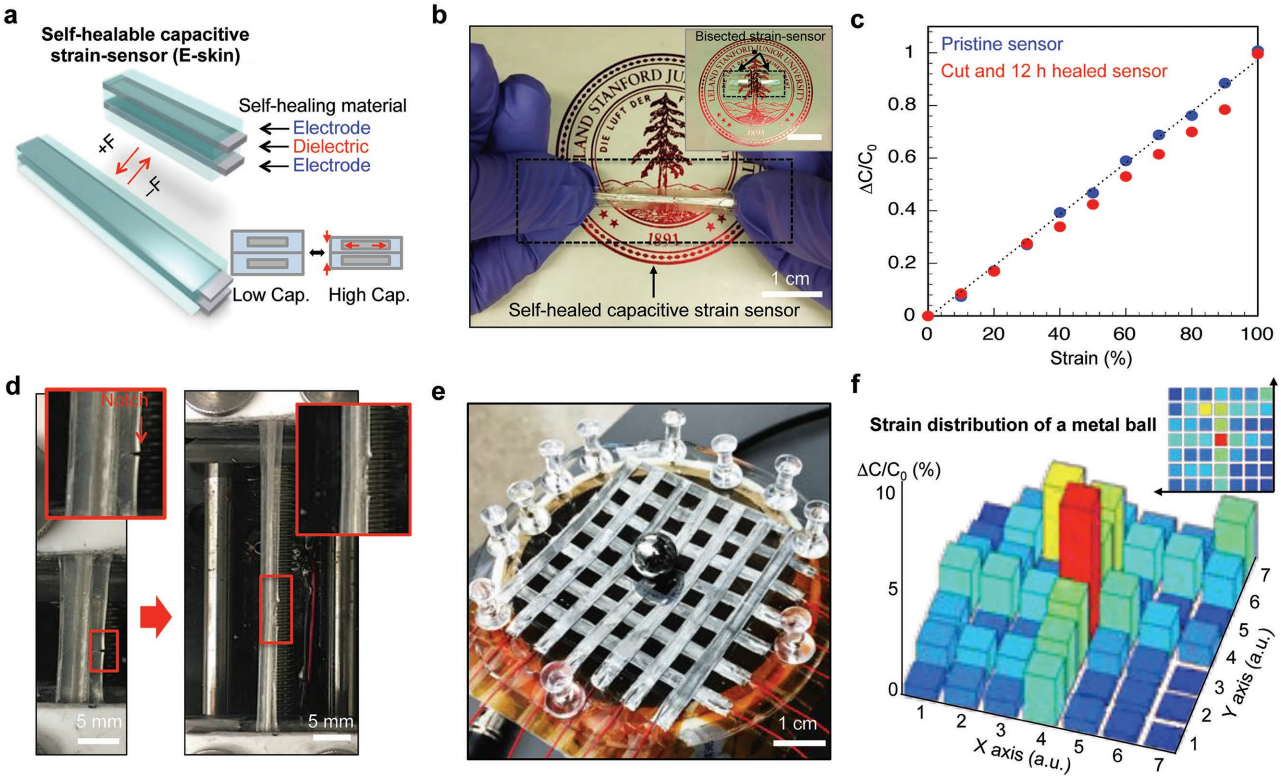

Figure 4. Highly stretchable and self-healable electronic skin. a) Schematic illustration of the strain-sensor structure. A strain sensor was fabricated by bonding two self-healing electrodes. b) Optical images of the cut strain sensor (inset), and the healed strain sensor maintains high stretchability. c) Capacitance change of strain-sensor by stretching with original sensor and 9 h healed sensor after damage. d) Optical images of a notched strain sensor on a stretching station. Optical image of a notched strain sensor after stretching. e) Optical image of a 7 × 7 strain-sensor array detecting the presence of a metal ball. f) Map of the strain distribution based on the change in capacitance by the weight of the metal ball (≈30 g).

e-skin is comparable to previously reported "ionic" skin[35] (Figure S19, Supporting Information). We observed a linear increment of capacitance (C) along with stretching, which matches well with the calculated values, $C = C_0\Delta L/L_0$, where L is the length of the strain sensor. We observed stable operation of our e-skin to 30% strain over 100 cycles (Figure S20, Supporting Information). The PDMS–$MDU_{0.4}$–$IU_{0.6}$ film exhibited viscoelastic behavior, limiting its strain sensing capability at high frequency. However, when our e-skin is conformably mounted on human skin, the viscoelastic behavior seems to disappear with the assistance of an elastic supporting substrate. For example, we observed that when the e-skin was mounted on a human finger, it could sensitively detect finger-bending motions with negligible hysteresis (Figure S21, Supporting Information). The e-skin is self-healable at room temperature when damaged or cut (Figure 4b,c). Further, even though some types of mechanical damage such as scratching and notching were made on the e-skin, it continued to operate because of the high toughness of the protective layer that prevented damage propagation under stretching (Figure 4d; Figure S22, Supporting Information). Thus, our e-skin is highly resistant to constant mechanical damage and provides time for the self-healing process to occur without interrupting its operation. The described approach is easily scalable, in which we demonstrated a wafer-scale 7 × 7 strain sensor array that is able to sense strain deformations induced by external stimuli (Figure 4e,f).

In summary, we describe a supramolecular polymer film, constructed via a mixture of strong and weak crosslinking hydrogen bonds. The resulting polymer possesses multiple desired mechanical properties for e-skin applications, e.g., stretchability, toughness, and autonomous self-healability even under water. Along with its ease in processability, we design and fabricate capacitive strain-sensing e-skin with high toughness and robustness against damage. The molecular design is simple and is expected to be applicable to various polymer structures. The described work provides molecular design guidelines for durable e-skin with self-healing properties.

Experimental Section

Preparation of PDMS–MPU_x–IU_{1-x} (x = 0, 0.2, 0.3, 0.4, 0.5, and 1) Films: Typical procedure of the preparation of PDMS–MPU_x–IU_{1-x} polymer films is as follows: 3–5 g of PDMS–MPU_x–IU_{1-x} was dissolved in 15 – 20 mL $CHCl_3$ and stirred at 50 °C. Resultant viscous solution was stirred for more than 3 h and was subsequently gradually cooled down to room temperature. The resultant solution was poured onto OTS-treated silicon substrates (4 in.) and dried at room temperature for 6 h followed by drying at 80 °C under reduced pressure (about 100 Torr) for 3 h. Polymer films were then peeled off after cutting in certain dimensions and ready for mechanical testing.

Mechanical and Self-Healing Tests: Mechanical-tensile-stress experiments were performed using an Instron 5565 instrument. At least three samples were tested for each type of polymer film. Tensile

experiments were performed under ambient conditions with samples with a width of 5 mm, a thickness of ≈0.5 mm, a length of 10 mm, and a controlled strain rate of 20 mm mm^{-1}. A sample with a length of 5 mm. a thickness ≈0.5 mm, and a width of 40 mm was used and for a notched sample a notch of 20 mm length was made in the middle of a strip of the film with a strain rate of 50 mm mm^{-1}. For self-healing tests, the polymer film was cut into two pieces and then the cut surfaces were put in contact. The polymer films were then healed at room temperatures for different periods. The healed polymer films were then stretched. The healing efficiency was defined as the ratio of strain at break between the healed film and the original film. Values of the Young's modules, maximum strain at break, and healing efficiencies were determined according to data of at least three trials.

Fabrication Process of Self-Healing Electrode and e-Skin: The self-healing electrode was fabricated by taking advantage of the moldable feature of the polymer at high temperature and its bonding property. A wafer-sized polymer film with 0.8 mm thickness on OTS-treated silicon substrate was prepared. The polymer film on substrate was pressed by Teflon mold at 80 °C and allowed to rest for 2 h. Then, after removing the Teflon mold, successful pattern with periodic polymer walls was confirmed and liquid metal alloy (EGaIn) was bladed onto the pattern by using small piece of polymer film and other polymer film with 0.3 mm thickness was subsequently put on patterned film with liquid metal as an encapsulation layer. The bonding process involves annealing at r.t. for 6 h after applying gentle pressure to keep the two pieces in good contact; robust self-healing electrode was obtained with stable interface. The electronic skin was fabricated by simply sandwiching a dielectric layer with two self-healing electrodes, in which the thickness of the dielectric layer was 330 µm.

Supporting Information

Supporting Information is available from the Wiley Online Library or from the author.

Acknowledgements

J.K. and D.S. contributed equally to this work. This work was supported by Samsung Electronics.

Conflict of Interest

The authors declare no conflict of interest.

Keywords

electronic skin, self-healable electronics, self-healing elastomer, toughness

Received: November 22, 2017
Revised: December 27, 2017
Published online: February 9, 2018

[1] a) A. Chortos, J. Liu, Z. Bao, *Nat. Mater.* **2016**, *15*, 937; b) Y. Liu, K. He, G. Chen, W. R. Leow, X. Chen, *Chem. Rev.* **2017**, *117*, 12893.

[2] a) D. H. Kim, N. S. Lu, R. Ma, Y. S. Kim, R. H. Kim, S. D. Wang, J. Wu, S. M. Won, H. Tao, A. Islam, K. J. Yu, T. I. Kim, R. Chowdhury, M. Ying, L. Z. Xu, M. Li, H. J. Chung, H. Keum, M. McCormick, P. Liu, Y. W. Zhang, F. G. Omenetto, Y. G. Huang, T. Coleman, J. A. Rogers, *Science* **2011**, *333*, 838; b) D.-H. Kim, J. Viventi, J. J. Amsden, J. Xiao, L. Vigeland, Y.-S. Kim, J. A. Blanco, B. Panilaitis, E. S. Frechette, D. Contreras, D. L. Kaplan, F. G. Omenetto, Y. Huang, K.-C. Hwang, M. R. Zakin, B. Litt, J. A. Rogers, *Nat. Mater.* **2010**, *9*, 511; c) D. Son, J. Lee, S. Qiao, R. Ghaffari, J. Kim, J. E. Lee, C. Song, S. J. Kim, D. J. Lee, S. W. Jun, S. Yang, M. Park, J. Shin, K. Do, M. Lee, K. Kang, C. S. Hwang, N. Lu, T. Hyeon, D.-H. Kim, *Nat. Nanotechnol.* **2014**, *9*, 397; d) J. Kim, M. Lee, H. J. Shim, R. Ghaffari, H. R. Cho, D. Son, Y. H. Jung, M. Soh, C. Choi, S. Jung, K. Chu, D. Jeon, S.-T. Lee, J. H. Kim, S. H. Choi, T. Hyeon, D.-H. Kim, *Nat. Commun.* **2014**, *5*, 5747; e) M. Kaltenbrunner, T. Sekitani, J. Reeder, T. Yokota, K. Kuribara, T. Tokuhara, M. Drack, R. Schwödiauer, I. Graz, S. Bauer-Gogonea, S. Bauer, T. Someya, *Nature* **2013**, *499*, 458.

[3] Z. Liu, D. Qi, G. Hu, H. Wang, Y. Jiang, G. Chen, Y. Luo, X. Loh,B. Liedberg, J. B. X. Chen, *Adv. Mater.* **2017**, *29*, 1704229.

[4] E. Palleau, S. Reece, S. C. Desai, M. E. Smith, M. D. Dickey, *Adv. Mater.* **2013**, *25*, 1589.

[5] B. C. Tee, C. Wang, R. Allen, Z. Bao, *Nat. Nanotechnol.* **2012**, *7*, 825.

[6] B. J. Blaiszik, S. L. B. Kramer, M. E. Grady, D. A. McIlroy, J. S. Moore, N. R. Sottos, S. R. White, *Adv. Mater.* **2012**, *24*, 398.

[7] Y. Li, S. Chen, M. Wu, J. Sun, *Adv. Mater.* **2012**, *24*, 4578.

[8] C. Gong, J. Liang, W. Hu, X. Niu, S. Ma, T. H. Hahn, Q. Pei, *Adv. Mater.* **2013**, *25*, 4186.

[9] J. Li, J. Liang, L. Li, F. Ren, W. Hu, J. Li, S. Qi, Q. Pei, *ACS Nano* **2014**, *8*, 12874

[10] Y. Li, S. Chen, M. Wu, J. Sun, *ACS Appl. Mater. Interfaces* **2014**, *6*, 16409.

[11] E. Ducrot, Y. Chen, M. Bulters, R. P. Sijbesma, C. Creton, *Science* **2014**, *344*, 186.

[12] J.-Y. Sun, X. Zhao, W. R. K. Illeperuma, O. Chaudhuri, K. H. Oh, D. J. Mooney, J. J. Vlassak, Z. Suo, *Nature* **2012**, *489*, 133.

[13] T. L. Sun, T. Kurokawa, S. Kuroda, A. B. Ihsan, T. Akasaki, K. Sato, M. A. Haque, T. Nakajima, J. P. Gong, *Nat. Mater.* **2013**, *12*, 932.

[14] J. A. Neal, D. Mozhdehi, Z. B. Guan, *J. Am. Chem. Soc.* **2015**, *137*, 4846.

[15] M. Guo, L. M. Pitet, H. M. Wyss, M. Vos, P. Y. Dankers, E. Meijer, *J. Am. Chem. Soc.* **2014**, *136*, 6969.

[16] F. Luo, T. L. Sun, T. Nakajima, T. Kurokawa, Y. Zhao, K. Sato, A. B. Ihsan, X. Li, H. Guo, J. P. Gong, *Adv. Mater.* **2015**, *27*, 2722.

[17] I. Jeon, J. Cui, W. R. Illeperuma, J. Aizenberg, J. J. Vlassak, *Adv. Mater.* **2016**, *28*, 4678.

[18] C.-H. Li, C. Wang, C. Keplinger, J.-L. Zuo, L. Jin, Y. Sun, P. Zheng, Y. Cao, F. Lissel, C. Linder, X.-Z. You, Z. Bao, *Nat. Chem.* **2016**, *8*, 618.

[19] W. Bai, Z. Jiang, A. Ribbe, S. Thayumanavan, *Angew . Chem., Int. Ed.* **2016**, *55*, 10707.

[20] T. F. A. De Greef, M. M. J. Smulders, M. Wolffs, A. P. H. J. Schenning, R. P. Sijbesma, E. W. Meijer, *Chem. Rev.* **2009**, *109*, 5687.

[21] Y. Yang, M. W. Urban, *Chem. Soc. Rev.* **2013**, *42*, 7446.

[22] P. Cordier, F. Tournilhac, C. Soulié-Ziakovic, L. Leibler, *Nature* **2008**, *451*, 977.

[23] S. R. White, N. Sottos, P. Geubelle, J. Moore, M. Kessler, S. Sriram, E. Brown, S. Viswanathan, *Nature* **2001**, *409*, 794.

[24] Y. Chen, A. M. Kushner, G. A. Williams, Z. Guan, *Nat. Chem.* **2012**, *4*, 467.

[25] M. Burnworth, L. Tang, J. R. Kumpfer, A. J. Duncan, F. L. Beyer, G. L. Fiore, S. J. Rowan, C. Weder, *Nature* **2011**, *472*, 334.

[26] X. Chen, M. A. Dam, K. Ono, A. Mal, H. Shen, S. R. Nutt, K. Sheran, F. Wudl, *Science* **2002**, *295*, 1698.

[27] B. Ghosh, M. W. Urban, *Science* **2009**, *323*, 1458.
[28] C. Wang, H. Wu, Z. Chen, M. T. McDowell, Y. Cui, Z. Bao, *Nat. Chem.* **2013**, *5*, 1042.
[29] H. Wang, B. Zhu, W. Jiang, Y. Yang, W. R. Leow, H. Wang, X. Chen, *Adv. Mater.* **2014**, *26*, 3638.
[30] M. D. Dickey, *Adv. Mater.* **2017**, *29*, 1606425.
[31] M. D. Dickey, *ACS Appl. Mater. Interfaces* **2014**, *6*, 18369.
[32] Y. Liu, M. Gao, S. F. Mei, Y. T. Han, J. Liu, *Appl. Phys. Lett.* **2013**, *103*, 064101.
[33] G. Li, X. Wu, D.-W. Lee, *Lab Chip* **2016**, *16*, 1366.
[34] J.-H. So, J. Thelen, A. Qusba, G. J. Hayes, G. Lazzi, M. D. Dickey, *Adv. Funct. Mater.* **2009**, *19*, 3632.
[35] J. Y. Sun, C. Keplinger, G. M. Whitesides, Z. Suo, *Adv. Mater.* **2014**, *26*, 7608.